

Seismic Detectability of a Subsurface Ocean on Europa

Robert L. Kovach

Department of Geophysics, Stanford University, Stanford, California 94305

E-mail: kov@pangea.stanford.edu

and

Christopher F. Chyba

SETI Institute, Mountain View, California 94043; and Department of Geological and Environmental Sciences, Stanford University, Stanford, California 94305

Received August 4, 2000; revised October 23, 2000

A seismometer placed on Jupiter's moon Europa can use passive monitoring to determine the presence or absence of a possible liquid water ocean beneath Europa's surface ice and estimates of the thickness of the ice shell itself. Using probable seismic velocities for Europa's ice it is demonstrated that surface waves propagating in the frequency band of 0.1 to 0.5 Hz (wave periods of 2 to 10 s) can discriminate ice shells varying from 5 to 20 km in thickness. Miniature, light-weight seismometers with appropriate sensitivities are available. © 2001 Academic Press

Key Words: Europa; ice; tectonics; instrumentation.

INTRODUCTION

The existence of a subsurface "ocean" of liquid water on Europa was suggested shortly after the flyby of the *Voyager I* spacecraft (Cassen *et al.* 1979). The groundbased spectroscopic signature of Europa is dominated by water ice (Clark *et al.* 1986), and interior models based on bulk density suggested there could be an outer layer of ice ~100 km thick overlying a rock/mantle interior, provided that Europa was a differentiated body (Cassen *et al.* 1979). Theoretical models indicated sufficient geothermal and tidal heating in Europa's subsurface to maintain much of this ice layer as liquid water beneath an outer layer of ice ~10 km thick (Cassen *et al.* 1979, 1980; Ross and Schubert 1987; Squyres *et al.* 1983; Ojakangas and Stevenson 1989). The paucity of craters on Europa's surface, combined with estimates of the comet impact rate in the jovian system, suggest that Europa's average surface age is ~10 Myr (Zahnle *et al.* 1998, 1999), indicating that Europa must be a geologically active world that resurfaces itself on this timescale.

Gravity measurements with the *Galileo* spacecraft indicate that Europa is in fact a differentiated body. Permissible first-order radial density models that do not violate mass and moment of inertia constraints indicate that Europa can have a combined

ice/liquid water shell ~80–170 km thick overlying a rocky mantle mixture of silicates and metals (Anderson *et al.* 1997, 1998).

Perhaps the most compelling evidence for a subsurface liquid water layer on Europa comes from recent magnetic field results (Khurana *et al.* 1998, Kivelson *et al.* 2000) that show the signal of an induced field at Europa. This signal requires the existence of a near-surface, global conducting layer, for which the most probable explanation is a global, salty ocean.

Consistent with this result, high-resolution images of Europa's surface show a variety of features that are interpretable as indicative of an ice shell overlying a subsurface liquid layer, including linear features, chaotic terrain, and small "ponds" (for summaries, see Greeley *et al.* (1998) and Pappalardo *et al.* (1999)). The orientation and relative age relationships of European lineaments is consistent with nonsynchronous rotation of an ice shell decoupled from a synchronously rotating interior by liquid water or ductile ice (Geissler *et al.* 1998). Other images show regions of chaotic terrain, where broken pieces of the surface seems to have "rafted" into new positions (Carr *et al.* 1998, Williams and Greeley 1998, Greenberg *et al.* 1999), cracks and extensional bands that likely were filled in with new, fluid material (Greenberg *et al.* 1998, Tufts *et al.* 2000), and cycloidal cracking explicable in terms of changing diurnal stress (Hoppa *et al.* 1999). Such geological features could have been formed in a thin (only a few kilometers thick) frozen crustal layer overlying liquid water (Greenberg *et al.* 2000), but solid-state explanations for many of them have also been suggested. The solid-state explanations typically involve diapirism within a thick (tens of kilometers thick) ice crust, possibly including bodies of melt or partial melt within the ice shell, overlying a liquid water ocean (Pappalardo *et al.* 1998, 1999; McKinnon 1998, 1999; Head *et al.* 1999; Collins *et al.* 2000).

All of this evidence, however, including the magnetic field results, is indirect in nature. The direct detection of a liquid water layer could be made by an orbiting altimeter or ice-penetrating radar. A laser altimeter could measure the tidal deformation of

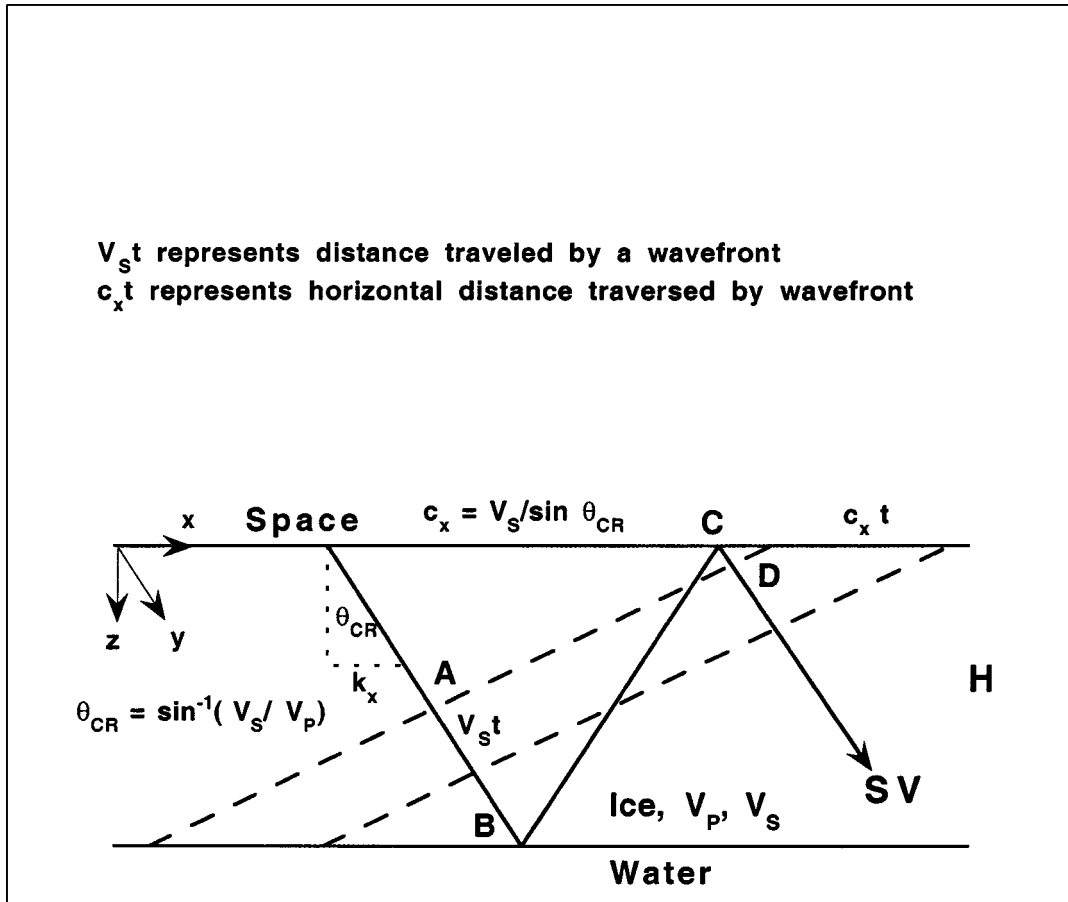


FIG. 1. Raypath diagram for vertically polarized (SV) waves critically reflected in an ice sheet on water.

Europa's surface; the amplitude of the time-varying tidal bulge will be more than an order of magnitude greater if Europa has an ice layer over liquid water (vertical deflection ~ 30 m) than it will be for solid ice (vertical deflection ~ 1 m). Since the tidal response depends on the product of the thickness and rigidity of the decoupled ice shell, Moore and Schubert (2000) argue that it will prove difficult to determine the thickness of the ice in this way. It is possible that a radar sounder could detect an ice/water interface on Europa directly, but this instrument could fail to penetrate an ice layer with sufficient conductivity or volumetric scattering. A radar instrument may well provide important information about subsurface structure, but cannot be counted on as an "ocean-detection" instrument (Chyba *et al.* 1998, Moore 2000).

Yet knowledge of the thickness of Europa's ice shell and the depth of its putative subsurface ocean has important implications for exobiology (Chyba 2000a, b; Greenberg *et al.* 2000; Gaidos and Nimmo 2000; Chyba and Phillips 2001). Here we demonstrate that one or more seismic sensors, emplaced on the European surface, could use passive monitoring not only to determine the presence or absence of a liquid water ocean, but also to estimate the thickness of the ice shell.

Both diurnal variation and nonsynchronous rotation can create significant stress fields in Europa's ice (Greenberg *et al.* 1998). Convection, density differences, and topographic differences may also contribute to the background stored stresses. Any of these may trigger or help trigger localized stress release on fractures (e.g., Hoppa *et al.* (1999)). This fracturing may be accompanied by detectable natural seismic signals. The natural quakes on Earth's Moon demonstrated a strong reproducibility and correlation with the tidal cycle (Toksöz *et al.* 1977). We anticipate that the alternating stress regimes caused by tidal flexing over each 3.55-day European tidal cycle will also trigger seismic activity.

Europa's surface is subject to comet and asteroid impacts (Zahnle *et al.* 1998, 1999), which would also result in seismic signals. However, the small-mass spectrum (and therefore frequency) of comet and asteroid impacts in the jovian system remains poorly known (see Pappalardo *et al.* (1999) for a review).

In this paper we demonstrate that simple passive seismic monitoring with a single 3-axis instrument placed on Europa's surface can yield information regarding the presence or absence of a liquid ocean beneath the surface ice layer, and provide estimates of the thickness of the ice layer itself.

Postulated Europa SH Waves Ice over Water

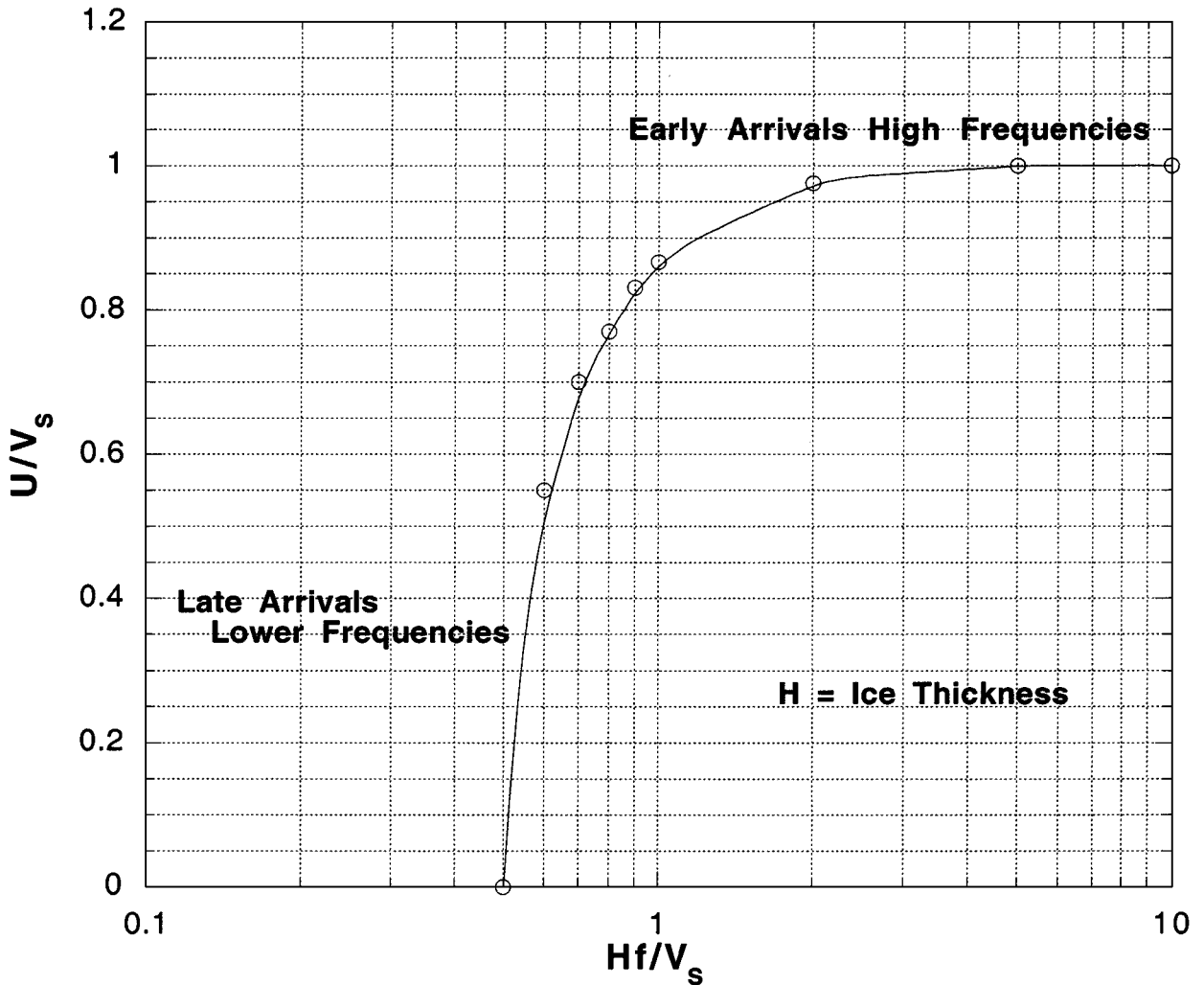


FIG. 2. Nondimensional group velocity as a function of nondimensional frequency for SH waves (Love waves) trapped in a floating ice sheet. V_s is the shear wave velocity in the ice. Observe the inverse dispersion in that higher frequencies arrive first (see text).

GENERAL COMMENTS ON SEISMIC WAVES

A few general comments are in order. Seismology makes use of the travel times of seismic body pulses and the dispersion of seismic surface waves to infer the internal velocity structure of a planetary body. Seismic body waves are of two types: compressional or longitudinal waves and shear or transverse waves. In a compressional wave the propagating displacement field varies in the direction of propagation. In contrast, a shear wave has its propagating displacement field varying at right angles to the direction of propagation. We further categorize shear waves into SV waves and SH waves. By defining the z axis as downward and placing the x - z plane along a great circle path between a source and receiver, shear wave polarizations can be defined. SV waves will have transverse displacements in the x - z plane and

are called vertically polarized shear waves. SH waves, horizontally polarized shear waves, will have their displacements in the y direction and thus be parallel to a planetary surface.

Surface waves offer the most promising tool for exploring Europa's outer layers. These waves propagate as Love or Rayleigh waves in a waveguide formed by velocity variations with depth. Since the wave propagation is dispersive the phase velocity, c , of propagation is dependent on frequency through a characteristic equation involving the velocity depth function. In other words, different wavelengths "see" different depths. The observed surface wave dispersion can be inverted to infer the variation of seismic wave velocity with depth. Love wave propagation can also be envisaged as SH waves trapped in a surface waveguide. Rayleigh wave propagation is more complicated involving P and SV waves trapped near the surface.

SEISMIC VELOCITIES IN ICE

Some terrestrial observations for the velocities of compressional (V_p) and shear waves (V_s) in glacier ice and on floating ice sheets are summarized in Table I. The data indicate average values of $V_p \sim 3.58$ km/s and $V_s \sim 1.66$ km/s. The temperature range of the reported observations is limited but the observations indicate that seismic velocities in ice increase as the temperature decreases. We are interested in values appropriate for the temperature conditions on Europa.

Proctor (1966) and Hobbs (1974) presented values for the dynamic compliance and stiffness constants of ice in the temperature range from 60 to 110 K. From these values the seismic velocities in ice can be determined. For hexagonal crystals, like ice, there are five independent stiffness or compliance constants that vary nonlinearly with respect to temperature. Hobbs (1974) calculated that the spatially averaged velocities of longitudinal and transverse waves in ice at 0 K are 4.2 and 2.1 km/s respectively. For ice at 110 K, the average surface temperature of Europa, the average values, using the technique described by Anderson (1963), with an ice density of 0.93 g cm^{-3} are 4.0 and 2.0 km/s. These values for the seismic velocities are about 5–10% greater than the velocities measured on terrestrial glaciers at temperatures of 256–273 K. All of the data for ice, over a wide temperature range, indicate that V_p varies in tandem with V_s as $V_p \sim 2V_s$. The calculated value of Poisson's ratio for ice is 0.35, higher than the value of 0.25 typically measured for terrestrial rocks. For Europa modeling purposes we shall adopt values of $V_p = 4.0$ km/s and $V_s = 2.0$ km/s. Contaminates, such as salts (McCord *et al.* 1999), are believed to be present in Europa's ice. The results of Khurana *et al.* (1998) and Kivelson *et al.* (2000) suggest that the salinity of Europa's ocean may be roughly comparable to that of Earth. Values of seismic velocities for terrestrial sea ice fall within the range of values observed on glaciers (Table I) and also indicate that $V_p \sim 2V_s$. Sea ice, with a salinity of 1%, at subfreezing temperatures has a density only 0.7% greater than that of pure ice (Anderson 1960). It is believed that at Europa's temperature any change in the assumed veloci-

ties, which are a function of the elastic moduli and the density, produced by salty contaminants can be taken to be minimal.

CRARY WAVES

A distinctive seismic wave may be observed on a floating ice sheet on Europa. This is the Crary wave, an unusual type of vertically polarized shear wave (Crary 1954), produced by critical angle multiple reflections at the upper and lower ice boundaries. Assume a SV wave traveling from left to right critically reflected at the upper space-ice and lower ice-water interface (Fig. 1). The critical angle of incidence θ_{cr} is equal to $\sin^{-1}(V_s/V_p)$. At this angle the incident SV wave is totally reflected back into the ice with a reversal of phase at both interfaces in its original form as an SV wave. At this angle of incidence on the boundaries the vertical displacement becomes zero.

We are interested in finding the SV wave frequency, f , which gives constructive interference between multiply reflected waves. Constructive interference will take place when the total wavelength path of a ray $ABCD$, corrected for phase shifts at the interfaces, is a multiple of a wavelength, λ , or

$$2H \cos \theta_{cr} - \lambda = n\lambda, \quad n = 1, 2, \dots \quad (1)$$

The second term allows for the phase reversals on reflection at the space-ice and water-ice interfaces. $\lambda = V/f$ where f is the frequency so that for $n = 1$ we have

$$H = V/f \cos \theta_{cr}. \quad (2)$$

The Crary wave is most easily seen on a radial component (longitudinal horizontal) seismic sensor, i.e., a sensor oriented with its axis along the path from the source to the receiver. Its horizontal phase velocity is $V_s/\sin \theta_{cr}$ so that the wave will arrive shortly after the first arrival compressional wave and before that of the horizontally polarized shear waves (SH).

Its frequency content is almost constant, being governed by constructive interference and as a result its characteristic

TABLE I
Longitudinal and Shear Velocities in Terrestrial Ice Sheets

Location	V_p (km/sec)	V_s (km/sec)	Temperature, °K	Reference
Austrian Alps	3.60	1.69	273	Mothes (1927, 1929)
	3.20	1.70	273	Köhler (1929)
Austrian Alps	3.58	1.67	273	Brockamp and Mothes (1930, 1931)
Grand Glacier d'Aletsch	3.57	1.67	273	Mothes (1929)
Ross Shelf Ice, Antarctica	3.36–3.90	0.9–1.58	?	Poulter (1947a, b)
Dronning Maud Land, Antarctica	3.80	?	?	Robin (1953)
West Greenland Icecap	3.80	1.91	268	Joset and Holtzscherer (1953)
West Greenland Icecap	3.82	1.92	256	Joset and Holtzscherer (1953)
Central Greenland Icecap	4.00	1.94	245	Joset and Holtzscherer (1953)
Fletcher's Ice Island, Arctic Ocean	3.35–3.78	1.71–1.84	?	Crary (1954)
Arctic Pack Ice	2.93–3.49	1.49–1.56	?	Oliver <i>et al.</i> (1934), Ewing and Crary (1934)

frequency is *immediately diagnostic of the ice thickness*. The ice thickness is equal to $V_s/f \cos \theta_{cr}$. For example, adopting values for Europa of $V_p = 4.0$ km/s and $V_s = 2.0$ km/s gives $\theta_{cr} = \sin^{-1}(V_s/V_p)$ of 30° . An ice thickness of 5 km would yield a characteristic frequency of 0.48 Hz, an ice thickness of 10 km 0.24 Hz. The seismic velocities in a European ice shell of unknown thickness will vary with depth controlled by the nonlinear temperature gradient within the ice. The resultant “ringing” frequency of the surface waveguide will still be proportional to a weighted average shear velocity as a function of depth and must lie within the bounds of 1.7 to 2.0 km/s.

SH WAVES OR LOVE WAVES

A special case of Love wave propagation will also take place in a floating ice sheet. In this case horizontally polarized shear waves are trapped and multiply reflected within the ice layer because of complete reflection at all angles of incidence at the upper and lower boundaries of the ice sheet. This condition arises because of the forced upper and lower boundary conditions of the vanishing of the tangential stresses and the absence of any rigidity modulus above and below the ice layer. Press and Ewing (1951) have shown that Love waves will propagate provided the following condition is met:

$$\tan \left[k_x H (c_x^2/V_s^2 - 1)^{1/2} \right] = 0. \quad (3)$$

H is the ice thickness, k_x is the horizontal wave number, c_x is the horizontal phase velocity, and V_s is the shear wave velocity in the ice. It can be seen that this expression will be satisfied if $k_x H (c_x^2/V_s^2 - 1)^{1/2} = n\pi$, where $n = 0, 1, \dots$

Making the substitution $V_s/c_x = \sin \theta$ and $k_x = 2\pi \sin \theta/\lambda$, where λ is the wavelength in the direction of propagation, we obtain the expression for constructive interference between multiple-reflected SH waves with an incident angle θ from (3) as

$$2H \cos \theta = n\lambda. \quad (4)$$

Since $c_x = 2\pi f/k_x$ the Love wave is dispersed in that different frequencies have different apparent velocities. For a dispersed wave train it is the group velocity $U = d(c_x k_x)/dk_x$ that controls the sequence of arrivals on a seismogram. From (3) we can show that $U = V_s \sin \theta = V_s^2/c_x$. Using the above relations we can compute a nondimensional group velocity dispersion curve given in Fig. 2. Because of the periodicity of the tangent function there are an infinite number of modes. Only the fundamental mode is shown in the figure.

The following features can be noted for Love wave propagation in a floating ice sheet. As $2\pi/\lambda \rightarrow \infty$ (i.e., very short wavelengths), $U \rightarrow V_s$ the velocity of shear waves in the ice layer. In other words the first arrivals are high-frequency waves that travel with the velocity V_s . With advancing time the wave frequency decreases until it reaches a cutoff frequency given by $V_s/2H$. This result is distinctly different to wave propagation

in an ice layer overlying a rocky substrate. In this case the finite, faster shear wave velocity in the substrate would produce normal dispersion with lower frequencies arriving first (Jobert 1953). Hence, we have our first simple diagnostic tool. *If Europa's outer shell is ice overlying liquid we would observe inverse dispersion with higher frequencies arriving first.* If a fluid substrate were absent the observed sequence of arrivals would exhibit normal dispersion. The nondimensional group velocity relation as a function of frequency can now be scaled using the thickness of the ice as a variable (Fig. 3). It can be seen that the steep portion of the dispersion curve will govern a portion of the arriving wave train. In other words, a large change in group velocity will occur for a very small change of frequency or wave period. Since group velocity is distance divided by the travel time of a wave of a given frequency the observational result is that a long, nearly sinusoidal wave train will be generated whose *predominant frequency is indicative of the ice thickness*. On Europa measuring the nearly constant frequency of this SH seismic wave will be a direct determination of the *average ice thickness* between a source and receiver.

One final aspect of the Love wave (surface wave) dispersion on Europa needs to be mentioned. For the floating ice sheet we have assumed for computational simplicity a plane layer approximation rather than a spherical shell. Europa's radius is comparable to that of the Earth's Moon so a plane layer approximation is adequate as long as the seismic wave periods do not exceed 25–30 s (Kovach and Press 1962). For ice shells ranging from 5 to 20 km in thickness the diagnostic wave periods range from 3 to 10 s and satisfy this requirement. In any case the effect of Europa's curvature would be to raise the values of the phase and group velocities at these longer periods by about 5%.

COUPLED P AND SV WAVES, RAYLEIGH WAVES

The complete wave propagation solution for coupled P and SV waves in a floating ice sheet is more complicated. Looking at short and long seismic wavelengths compared to the thickness of the floating ice sheet we can draw some conclusions for these limiting cases. For wavelengths that are intermediate in dimension to the ice thickness, the wave propagation velocity will become a complex number because attenuation is taking place as a result of wave radiation from the ice sheet into the water. This means that waves will be dispersive but selectively attenuated. For short wavelengths the seismic waves will propagate with the Rayleigh velocity, $0.9 V_s$, at the top of the ice layer and the Stoneley wave velocity, $0.87\alpha_2$, at the ice–fluid interface (α_2 is the compressional wave velocity in the fluid substrate). For long wavelengths the waves will propagate as flexural waves.

The important conclusion is that *simple seismic wave monitoring in the frequency band from 0.08 to 10 Hz (wave periods of 0.1 to 12.5 s) will be useful for discriminating thickness of a European ice shell ranging from kilometers to tens of kilometers*. In addition, straightforward measurements of S minus P-wave arrival times, which are directly proportional to the distance

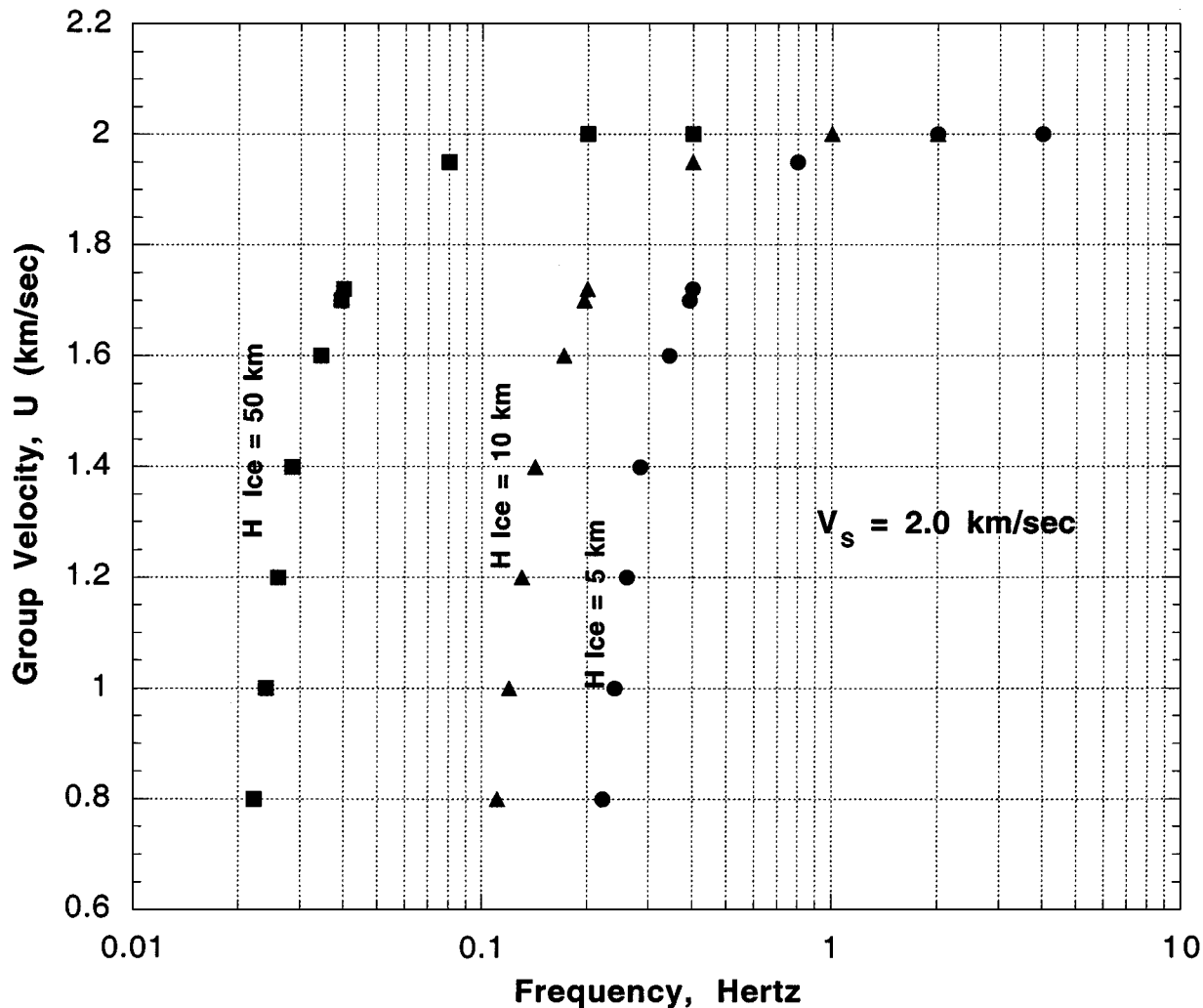


FIG. 3. Group velocity versus frequency for Love waves in a floating ice sheet of various thicknesses. H is the thickness of the ice.

from any natural tectonic event, should allow a first-order radial velocity mode for Europa to be determined.

Terrestrial ice tremors, which resemble miniature earthquakes, are produced by the fracturing of ice under various stresses (Crary 1954, 1955). Usually P and SH waves are well defined. The SH wave, as described earlier, shows a dispersed wave train with the initial impulse arriving at the velocity of the transverse waves. The main causes of internal fracturing and cracking on terrestrial lake ice sheets are thermal effects that often produce an audible signal similar to a rifle shot or the Doppler effect of a moving sound source.

SEISMIC INSTRUMENTATION

Any seismic detector to be used on Europa should be a 3-axis instrument. A 3-axis seismometer has the following advantages:

(1) The polarization of the seismic signal can be determined. This allows compressional, shear, and surface waves to be unambiguously identified.

(2) The angle of emergence of the seismic wave can be determined. This is relevant to determining the location of any quake and unraveling the structure of the interior.

(3) Love-type surface waves (SH) have no vertical component of motion and can be readily identified by component rotation.

A few general comments concerning the sensitivities and frequency response of seismometers are in order. Figure 4 is a plot of the acceleration sensitivity of various planetary seismometers in units of the Earth's gravitational acceleration, 980 cm/s^2 , versus the wave period of an input seismic signal. The response to ground velocity or ground displacement is obtained by dividing acceleration by the angular frequency ω or ω^2 respectively. The governing factor for any seismometer operation is the ambient background noise level. On the Earth, wind, cultural effects, and the cyclical tidally driven beating of the oceans on the continents govern this background noise level. Seismic stations operated at terrestrial coastal locations or on islands are always noisier than stations located farther inland from the coast. The curve marked

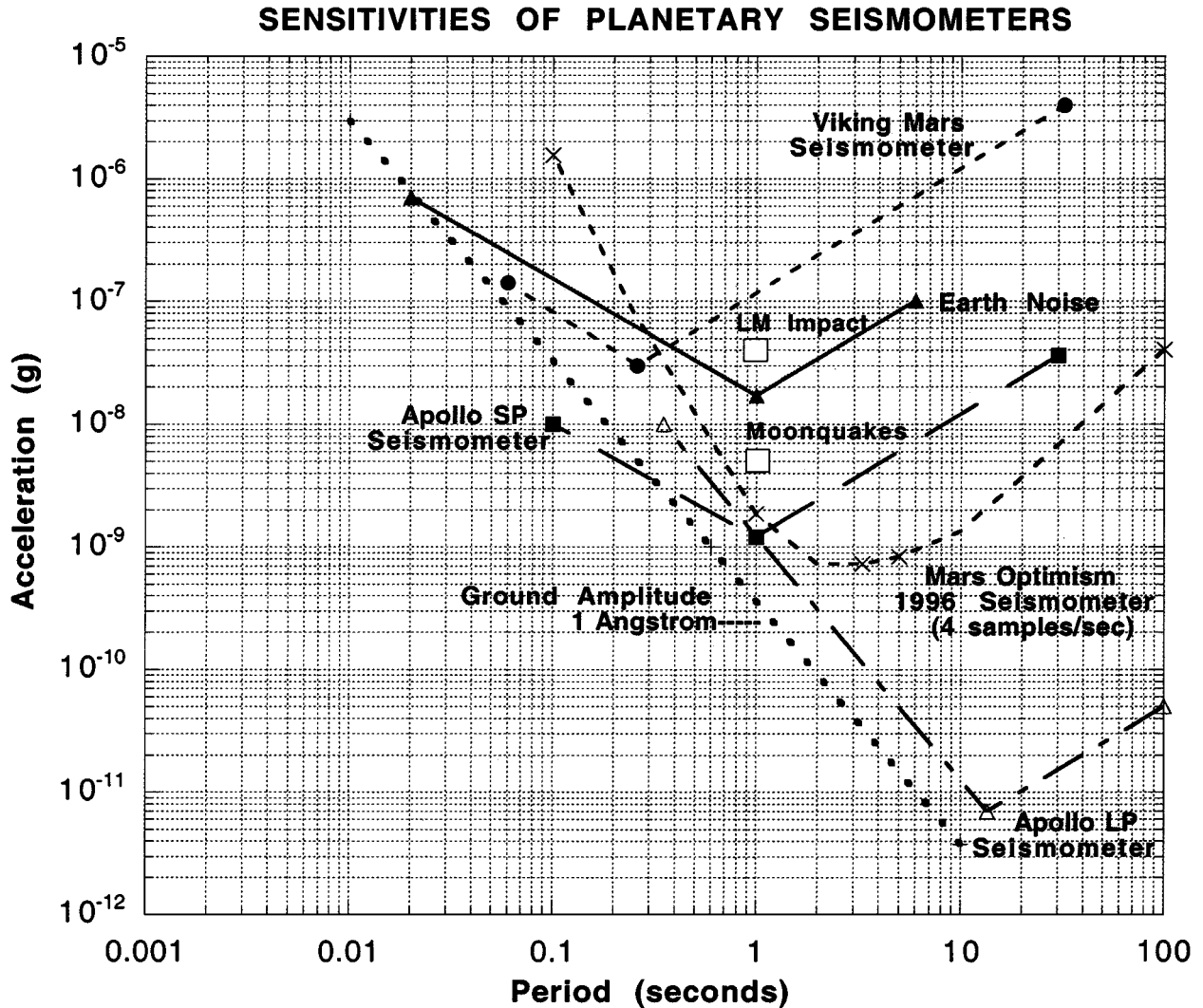


FIG. 4. Comparison of the acceleration sensitivity for various planetary seismometers.

Earth noise in Fig. 4 represents an “average” level of Earth noise and effectively sets the detection threshold or operational sensitivity of any Earth seismometer. The noise level on the Earth’s Moon was far below that of any Earth site and frequently below the threshold sensitivity of the Apollo long-period seismometer (3 \AA at 1 Hz or $1.2 \times 10^{-9} \text{ g}$). The leftmost line decreasing to the right (a slope of $+2$ with respect to ω) gives a reference input ground amplitude of 0.1 nm or 1 \AA . Shown for reference in Fig. 3 are the peak-to-peak amplitude observed for the Apollo 12 lunar module impact at a distance of 75.9 km (10 nm at 1 Hz) and typical amplitudes of moonquakes ($<2 \text{ nm}$ at 1 Hz).

Miniature seismometers for use on planetary missions are now available with sensitivities close to that achieved by the much heavier Apollo short- and long-period seismometers that were emplaced on the Earth’s Moon. For example, the Mars Optimism seismometer, built but not flown on a Mars mission, weighed 405 g with a volume of 729 cm^3 . A dual sensor was utilized: a velocity transducer for measurements in the period range from

0.5 to 10 s and a ground displacement transducer in the band from 5 to 50 s . Because the transducers possessed a very high value for the generator constant the overall resolution was more than 100 times better than that of the *Viking Mars* seismometer at corresponding wave periods (Lognonné *et al.* 1998). Electronics for A/D conversion, health and temperature monitoring, and a modest amount of data memory required additional weight, comparable to that of the seismic sensor itself.

With only a single seismic station on Europa the determination of the basic parameters of a natural event produced by an external impact or a tectonic quake, including distance, time of origin, and source nature and strength will be difficult but not impossible. On the Earth’s Moon meteoroid impacts and moonquakes were identified by examining seismic signature characteristics such as waveform matching, energy comparisons in waveforms, and coherence between signals. The time of occurrence of natural tectonic events at apogee and perigee was also a useful criteria.

The large *a priori* unknowns on Europa that will govern at what detection sensitivity a seismometer can be operated are the ambient seismic background noise and the expected rich source of noise generated by the landed spacecraft itself. Sources might be valve chatter, fuel venting, thermoelastic stress relief, and vibrations produced, for example, by movement of a camera. Such noises hopefully are of short duration, infrequent, and distinctive and occur at predictable times. Because these signals will complicate routine listening they need to be recognized so that separation can be made from signals produced by events of natural origin. Distinct advantages to seismic monitoring could be gained if the seismometer were part of a penetrator package positioned into the icy surface of Europa. It seems likely, however, that a European seismometer could be operated at near lunar sensitivities.

ACKNOWLEDGMENTS

The thoughtful reviews of Don L. Anderson and Gregory Hoppa are appreciated.

REFERENCES

- Anderson, D. L. 1960. The physical constants of sea ice. *Research (London)* **13**, 310–318.
- Anderson, D. L., R. L. Kovach, G. Latham, F. Press, M. N. Toksöz, and G. Sutton 1972. Seismic investigations: The Viking Mars Lander. *Icarus* **16**, 205–216.
- Anderson, D. L., W. F. Miller, G. V. Latham, Y. Nakamura, M. N. Toksöz, A. M. Dainty, F. K. Duennenbier, A. R. Lazarewicz, R. L. Kovach, and T. C. D. Knight 1977. Seismology on Mars. *J. Geophys. Res.* **82**, 4524–4546.
- Anderson, J. D., E. L. Lau, W. L. Sjogren, G. Schubert, and W. B. Moore 1997. Europa's differentiated internal structure: Inferences from two Galileo encounters. *Science* **176**, 1236–1239.
- Anderson, J. D., G. Schubert, R. A. Jacobsen, E. L. Lau, and W. B. Moore 1998. Europa's differentiated internal structure: Inferences from four Galileo encounters. *Science* **281**, 2019–2022.
- Anderson, O. L. 1963. A simplified method for calculating the DEBYE temperature from elastic constants. *J. Phys. Chem. Solids* **24**, 969–917.
- Brockamp, B., and H. Mothes 1930. Seismische Untersuchungen auf dem Pasterzegletscher. *Z. fur Geophys.* **6**, 482–500.
- Brockamp, B., and H. Mothes 1931. Seismische Untersuchungen auf dem Pasterzegletscher, II. *Z. Geophys.* **7**, 232–240.
- Carlson, R. W., R. E. Johnson, and M.S. Anderson 1999. Sulfuric acid on Europa and the radiolytic sulfur cycle. *Science* **286**, 97–99.
- Carr, M. H., M. J. S. Belton, C. R. Chapman, M. E. Davies, P. Geissler, R. Greenberg, A. S. McEwen, B. R. Tufts, R. Greeley, and R. Sullivan 1998. Evidence for a subsurface ocean on Europa. *Nature* **391**, 363–365.
- Cassen, P., S. J. Peale, and R. T. Reynolds 1980. Tidal dissipation in Europa: A correction. *Geophys. Res. Lett.* **7**, 987–988.
- Cassen, P., R. T. Reynolds, and S. J. Peale 1979. Is there liquid water on Europa? *Geophys. Res. Lett.* **6**, 731–734.
- Chyba, C. F. 2000a. Energy for microbial life on Europa. *Nature* **403**, 381–382.
- Chyba, C. F. 2000b. Correction: Energy for microbial life on Europa. *Nature* **406**, 368.
- Chyba, C. F., and C. B. Phillips 2001. Possible ecosystems and the search for life on Europa. *Proc. Natl. Acad. Sci. USA*, in press.
- Chyba, C. F., S. J. Ostro, and B. C. Edwards 1998. Radar detectability of a subsurface ocean on Europa. *Icarus* **134**, 292–302.
- Clark, R. N., F. P. Fanale, and M. J. Gaffey 1986. Surface composition of natural satellites. In *Satellites* (J. A. Burns and M. S. Matthews, Eds.), pp. 437–491. Univ. of Arizona Press, Tucson.
- Collins, G. C., J. W. Head, R. T. Pappalardo, and N. A. Spaun 2000. Evaluation of models for the formation of chaotic terrain on Europa. *J. Geophys. Res.* **105**, 1709–1716.
- Crary, A. P. 1954. Seismic studies on Fletcher's Ice Island, T-3. *Trans. Am. Geophys. Union* **35**, 293–300.
- Crary, A. P. 1955. A brief study of ice tremors. *Bull. Seismol. Soc. Am.* **45**, 1–9.
- Ewing, M., and A. P. Crary 1934. Propagation of elastic waves in ice, II. *Physics* **5**, 181–184.
- Gaidos, E. J., and F. Nimmo 2000. Tectonics and water on Europa. *Nature* **405**, 637.
- Geissler, P. E., R. Greenberg, G. Hoppa, P. Helfenstein, A. McEwen, R. Pappalardo, R. Tufts, M. Ockert-Bell, R. Sullivan, and R. Greeley 1998. Evidence for non-synchronous rotation of Europa. *Nature* **391**, 368–370.
- Greeley, R., R. Sullivan, J. Klemaszewski, K. Homan, J. W. Head III, R. T. Pappalardo, J. Veveřka, B. E. Clark, T. V. Johnson, K. P. Klaosen, M. Belton, J. Moore, E. Asphaug, M. H. Carr, G. Neukum, T. Denk, C. R. Chapman, C. B. Pilcher, P. E. Geissler, R. Greenberg, and R. Tufts 1998. Europa: Initial Galileo geological observations. *Icarus* **135**, 4–24.
- Greenberg, R., P. Geissler, G. Hoppa, B. R. Tufts, D. D. Durda, R. Pappalardo, J. W. Head, R. Greeley, R. Sullivan, and M. H. Carr 1998. Tectonic processes on Europa: Tidal stresses, mechanical response, and visible features. *Icarus* **135**, 64–78.
- Greenberg, R., P. Geissler, B. R. Tufts, and G. V. Hoppa 2000. Habitability of Europa's crust: The role of tidal-tectonic processes. *J. Geophys. Res.* **105**, 17,551–17,562.
- Greenberg, R., G. V. Hoppa, B. R. Tufts, P. Geissler, and J. Riley 1999. Chaos on Europa. *Icarus* **141**, 263–286.
- Head, J. W., R. T. Pappalardo, and R. J. Sullivan 1999. Europa: Morphologic characteristics of ridges and triple bands from Galileo data (E4 and E6) and assessment of a linear diapirism model. *J. Geophys. Res.* **104**, 24,223–24,236.
- Hobbs, P. V. 1974. *Ice Physics*. Clarendon Press, Oxford.
- Hoppa, G. V., B. R. Tufts, R. Greenberg, and P. E. Geissler 1999. Formation of cycloidal features on Europa. *Science* **285**, 1899–1902.
- Jobert, N. 1953. Dispersion des ondes de surface dans la couche superficielle du glacier du Groenland. *Ann. Geophys.* **9**, 345–357.
- Joset, A., and J. Holtzschcher 1953. Etude des vitesses de propagation des ondes seismiques sur l'inlandsis du Groenland. *Ann. Geophys.* **9**, 330–344.
- Khurana, K. K., M. G. Kivelson, D. J. Stevenson, G. Schubert, C. T. Russell, R. T. Walker, and C. Polanskey 1998. Induced magnetic fields as evidence for sub-surface oceans in Europa and Callisto. *Nature* **395**, 777–780.
- Kivelson, M. G., K. K. Khurna, C. T. Russell, M. Volwerk, R. J. Walker, and C. Zimmer 2000. Galileo magnetometer measurements: A stronger case for subsurface ocean at Europa. *Science* **289**, 1340–1343.
- Köhler, R. 1929. Beobachtungen an Profilen auf See-Eis. *Z. Geophys.* **5**, 314–316.
- Kovach, R. L., and F. Press 1962. Lunar seismology. Jet Propulsion Laboratory Technical Report 32–328.
- Lognonné, P., and 14 colleagues 1998. The seismic OPTIMISM experiment. *Planet. Space Sci.* **46**, 739–747.
- McCord, T. B., G. B. Hansen, D. L. Matson, T. V. Johnson, J. K. Crowley, F. P. Fanale, R. W. Carlson, W. D. Smythe, P. D. Martin, C. A. Hibbitts, J. C. Granahan, and A. Ocampo 1999. Hydrated salt minerals on Europa's surface from the Galileo near-infrared mapping spectrometer (NIMS) investigation. *J. Geophys. Res.* **104**, 11,827–11,851.
- McKinnon, W. B. 1998. Geodynamics of icy satellites. In *Solar System Ices* (B. Schmitt, C. de Bergh, and M. Festou, Eds.), pp. 525–550. Kluwer, Dordrecht.

- McKinnon, W. B. 1999. Convective instability in Europa's floating ice shell. *Geophys. Res. Lett.* **26**, 951–954.
- Moore, J. C. 2000. Models of radar absorption in European ice. *Icarus* **147**, 292–300.
- Moore, W. B., and G. Schubert 2000. The tidal response of Europa. *Icarus* **147**, 317–319.
- Mothes, H. 1927. Seismische Dickenmessungen von Gletschereis. *Z. Geophys.* **3**, 121–134.
- Mothes, H. 1929. Neue Ergebnisse der Eisseismik. *Z. Geophys.* **5**, 314–316.
- Ojakangas, G. W., and D. J. Stevenson 1989. Thermal state of an ice shell on Europa. *Icarus* **81**, 220–241.
- Oliver, J., A. P. Cray, and R. Cotell 1954. Elastic waves in Arctic pack ice. *Trans. Am. Geophys. Union* **35**, 282–292.
- Pappalardo, R. T., J. W. Head, R. Greeley, R. J. Sullivan, C. Pilcher, G. Schubert, W. B. Moore, M. H. Carr, J. M. Moore, and M. J. S. Belton 1998. Geological evidence for solid-state convection in Europa's ice shell. *Nature* **391**, 365–367.
- Pappalardo, R. T., and 31 colleagues 1999. Does Europa have a subsurface ocean? Evaluation of the geological evidence. *J. Geophys. Res.* **104**, 24,015–24,055.
- Poulter, T. C. 1947a. Seismic measurements on the Ross Shelf Ice. *Trans. Am. Geophys. Union* **28**, 162–170.
- Poulter, T. C. 1947b. Seismic measurements on the Ross Shelf Ice. *Trans. Am. Geophys. Union* **28**, 367–384.
- Press, F., and M. Ewing 1951. Propagation of elastic waves in a floating ice sheet. *Trans. Am. Geophys. Union* **32**, 673–679.
- Proctor, T. M. 1966. Low-temperature speed of sound in single-crystal ice. *J. Acoust. Soc. Am.* **39**, 972–977.
- Robin, G. Q. 1953. Measurements of ice thickness in Dronning Maud Land, Antarctica. *Nature* **171**, 55.
- Ross, M., and G. Schubert 1987. Tidal heating in an internal ocean model of Europa. *Nature* **325**, 132–134.
- Shaw, G. H. 1986. Elastic properties and equation of state of high pressure ice. *J. Chem. Phys.* **84**, 5862–5868.
- Squyres, S. W., and S. Croft 1986. The tectonics of icy satellites. In *Satellites* (J. Burns and M. Matthews, Eds.), pp. 293–341. Univ. of Arizona Press, Tucson.
- Squyres, S. W., R. T. Reynolds, and P. M. Cossen 1983. Liquid water and active resurfacing on Europa. *Nature* **301**, 225–226.
- Sullivan, R., R. Greeley, K. Homan, J. Klemaszewski, M. J. S. Belton, M. H. Carr, C. R. Chapman, R. Tufts, J. W. Head III, and R. Pappalardo 1998. Episodic plate separation and fracture infill on the surface of Europa. *Nature* **391**, 371–373.
- Toksöz, M. N., N. R. Goins, and C. H. Cheng 1977. Moonquakes: Mechanisms and relation to tidal stresses. *Science* **196**, 979–981.
- Tufts, B. R., R. Greenberg, G. Hoppa, and P. Geissler 2000. Lithospheric dilation on Europa. *Icarus* **146**, 75–97.
- Williams, K. K., and R. Greeley 1998. Estimates of ice thickness in the Conamara Chaos region of Europa. *Geophys. Res. Lett.* **25**, 4273–4276.
- Zahnle, K., L. Dones, and H. F. Levison 1998. Cratering rates on the Galilean satellites. *Icarus* **136**, 202–222.
- Zahnle, K., H. Levison, L. Dones, and P. Schenk 1999. Cratering rates in the outer Solar System. In *Lunar and Planetary Science* 31st, Abstract 1776. Lunar and Planetary Institute, Houston. [CD-ROM]